A new species of *Papiliomyces* (Clavicipiteae, Hypocreales) from China

Yan Zhang[‡], TingChi Wen[‡,§,|], Yuanpin Xiao[¶,§], Yu Yang[|], Xingcan Peng[¶]

‡ College of Pharmacy, Guizhou University, Guiyang, China
§ Engineering Research Center of Southwest Bio-Pharmaceutical Resources, Ministry of Education, Guizhou University, Guiyang, China
| The Mushroom Research Centre, Guizhou University, Guiyang, China
¶ Center of Excellence in Fungal Research, and School of Science, Mae Fah Luang University, Chiang Rai, Thailand

Corresponding author: TingChi Wen (tingchiwen@yahoo.com)

Academic editor: Danny Haelewaters

Abstract

Background

Papiliomyces (Hypocreales, Sordariomycetes) was introduced to accommodate two species: *Papiliomyces liangshanensis* and *Papiliomyces shibinensis*. Later, *Papiliomyces liangshanensis* was renamed *Ophiocordyceps liangshanensis*. However, the *Papiliomyces liangshanensis* molecular data (Nepalese) used to establish the *Papiliomyces* genus was different from *Ophiocordyceps liangshanensis* (China) strains.

New information

This paper describes a new species, *Papiliomyces longiclavatus*, found in Yangchang District, Guiyang City, Guizhou Province, China. It is proposed, based on morphology and multilocus phylogeny (ITS, SSU, LSU, *TEF1*, *RPB1* and *RPB2*). The new species is phylogenetically most closely related to *Papiliomyces liangshanensis* (Nepalese collections). However, *Papiliomyces liangshanensis* (Nepalese collections) requires morphological details and additional detection. The new species differs from other *Papiliomyces* species in having robust stroma with completely immersed perithecia, multi-septate ascospores, cylindrical secondary ascospores, two types of phialides and two types of conidia:longer α-conidia and longer β-conidia.

Keywords

Papiliomyces, molecular phylogeny, one new species, taxonomy

Introduction

Fungi are amongst the most important organisms, influencing human activities and playing a crucial role in ecosystems (Mueller and Schmit 2007). About 2000 species of fungi are being described annually (Cheek et al. 2020). Entomopathogenic fungi have received great attention due to their ecological, economic and medical applications (Yang et al. 2021). However, the diversity of entomopathogenic fungi necessitates additional research.

Sung et al. (2007a) introduced the genus *Metacordyceps* to accommodate some species of *Cordyceps*, characterised by solitary to multiple stromata, simple to branched, with a fleshy or tough whitish stipe, strongly pigmented green to yellow cylindrical to enlarged fertile part and superficial perithecia partially or completely immersed in stroma (Sung et al. 2007a, Kepler et al. 2012a). Based on the generated DNA sequences and multi-gene phylogenetic evidence, Sung et al. (2007a) reclassified some species from *Metacordyceps* to *Papiliomyces*, such as *Metacordyceps liangshanensis* and *Metacordyceps shibinensis*. This was utilised in the Outline of Ascomycota (Wijayawardene et al. 2018).

The genus *Papiliomyces* was proposed by Mongkolsamrit et al. (2020) in *Clavicipiteae* family (Hypocreales, Sordariomycetes), based on phylogenetic analyses to accommodate two species: *Papiliomyces liangshanensis* (Nepalese collections) and *Papiliomyces shibinensis* (China). However, based on morphology and phylogenetic analyses, the type species, *Papiliomyces liangshanensis*, was recombined into *Ophiocordyceps* (Wang et al. 2021). The genus name originated from the Latin word 'papilio', meaning butterfly or moth (Mongkolsamrit et al. 2020). The primary characteristics of the teleomorph of *Papiliomyces* are solitary to multiple (branched and robust to wiry stromata), superficial perithecia to completely immersed in the stroma, ampulliform, ellipsoid to ovoid, asci cylindrical and ascospores whole with septation or breaking into cylindrical part-spores (Kepler et al. 2012a, Kepler et al. 2012b, Mongkolsamrit et al. 2020, Wang et al. 2021).

Through culturing and molecular approaches, *Metarhizium* has been linked to *Metacordyceps* as sexual states (Kepler et al. 2014). However, they are forming distinct branches in the phylogenetic tree. Moreover, *Metacordyceps* is different from *Metarhizium* in producing superficial perithecia and a wiry, branched stromata or a white to faint yellow robust stroma (Zang et al. 1982, Sung et al. 2007b, Wen et al. 2015, Mongkolsamrit et al. 2020). Sexual morphs of *Metarhizium* produce semi-immersed to completely immersed perithecia on a robust and almost fleshy dark green or purplish stroma (Sorokin 1883, Sung et al. 2007a, Kepler et al. 2012a). Phylogenetically, the genus is closely related to *Purpureomyces* and *Keithomyces* (Mongkolsamrit et al. 2020). The three species of *Purpureomyces* (Hywel-Jones 1994, Kepler et al. 2012a, Kepler et al. 2014) differ from *Papiliomyces* spp. in that they can produce fleshy, purple stromata and the ascomata are obliquely embedded in the stroma (Mongkolsamrit et al. 2020).

Keithomyces includes three species primarily isolated from soil, producing *Paecilomyces* -like asexual morphs, conidiophores with divergent whorls of two to four phialides and echinulate to aciculate conidia (Mongkolsamrit et al. 2020).

In this study, a new species, *Papiliomyces longiclavatus* is introduced, based on the morphology and phylogenetic analysis of a six-locus dataset.

Materials and methods

Sample collection and morphological characteristic examination

The specimens were collected from Yangchang Town, Wudang District, Guiyang City, Guizhou Province, China on 14 June 2020. They were stored in plastic containers at low temperature and transported to the laboratory for identification. The macro-morphological characteristics were described, based on fresh material and on the photographs provided here. Fresh specimens were used to isolate the fungus through the tissue culture method in a potato dextrose agar (PDA) medium. Herbarium materials were deposited at Guizhou University (GACP) and Kunming Institute of Botany, Chinese Academy of Sciences (HKAS). For micro-morphological examination, fruiting bodies and living culture mycelia were examined using a stereo dissecting microscope (Leica S9E). Hand sections of fruiting structures were mounted in water for microscopic study and photomicrography. The microcharacteristics of the fungi were examined under a Leica DM2500 compound microscope and photographed. Facesoffungi and Index Fungorum numbers were provided as explained by Jayasiri et al. (2015) and Index Fungorum (http://indexfungorum.org, accessed 6 April 2023).

DNA extraction, PCR amplification and sequencing

Dried specimens were used to extract genomic DNA using the EZgene TM Fungal gDNA Kit (Biomiga, CA, USA) according to the manufacturer's instructions. The extracted DNA was stored at -20°C. Reaction mixtures (25 µl) contained 2 µl template DNA (ca. 10 ng), 11 µl distilled water, 1 µl (10 µM) of each primer and 10 µl 2x Taq PCR StarMix with Loading Dye (GenStar). The primers for amplifying and sequencing were ITS5 and ITS4 for the internal transcribed spacer gene region (ITS) (White et al. 1990), LR0R and LR5 for the partial large subunit rDNA gene region (LSU) (Vilgalys and Hester 1990, Hopple 1994), NS1 and NS4 for the ribosomal small subunit rDNA gene region (SSU) (White et al. 1990), EF1-983F and EF1-2218R for the partial translation elongation factor 1-alpha gene region (*TEF1*) (Sung et al. 2007b), CRPB1 and RPB1Cr for the partial RNA polymerase II largest subunit gene region (*RPB1*) (Castlebury et al. 2004) and RPB2-5F2 and RPB2-7Cr for the partial RNA polymerase II second largest subunit gene region (*RPB2*) (Liu et al. 1999, O'Donnell et al. 2007). The PCR amplification conditions were the following: for ITS, initial denaturation at 94°C for 3 min, followed by 33 cycles of 94°C for 30 s, 51°C for 50 s and 72°C for 45 s and final extension of 72°C for 10 min; for LSU and SSU, initial denaturation at 94°C for 3 min, followed by 33 cycles at 94°C for 30 s, 51°C for 30 s and 72°C for 2 min and final extension of 72°C for 10 min; for *TEF1*, initial

denaturation at 94°C for 3 min, followed by 33 cycles of 94°C for 30 s, 58°C for 50 s and 72°C for 1 min and final extension of 72°C for 10 min; for *RPB1*, initial denaturation at 94°C for 3 min, followed by 33 cycles of 94°C for 1 min, 52°C for 1 min and 72°C for 1 min and final extension at 72°C of 10 min; and for *RPB2*, initial denaturation at 94°C for 3 min, followed by 33 cycles of 94°C for 30 s, 54°C for 40 s and 72°C for 80 s and final extension of 72°C for 10 min. The amplified PCR products were verified by 1% agarose gel electrophoresis stained with ethidium bromide in 1x TBE. They were directly sequenced with the above-mentioned primers by Sangon Biotech (Shanghai) Co., Ltd., Shanghai, China.

Sequence alignment and phylogenetic analyses

Reference sequences were downloaded from NCBI GenBank, https://www.ncbi.nlm.nih.gov/genbank/ (Table 1). BioEdit (Alzohairy 2011) was used to assemble downloaded and newly-generated sequences. Sequences were aligned by locus with MAFFT version 7 (Katoh and Standley 2013) (https://mafft.cbrc.jp/alignment/server/) and trimmed using TrimAl version 1.3 (Capella-Gutiérrez et al. 2009). FasParser was used to splice the ITS, SSU, LSU, *TEF1*, *RPB1* and *RPB2* sequences (Katoh and Standley 2013). Gaps were considered as missing data.

Maximum Likelihood (ML) analyses were performed using IQ-TREE 2 (Minh et al. 2020) under partitioned models. The built-in ModelFinder (Kalyaanamoorthy et al. 2017) was used to select appropriate models for each of the six loci. Branch support was estimated using 1000 ultrafast bootstrap (UFBoot2) replicates (Hoang et al. 2018). For Bayesian analysis (BI), MrBayes version 3.2.7 (Ronquist et al. 2012) was utilised to evaluate posterior probabilities (PP) using Markov Chain Monte Carlo sampling (MCMC). MrMTgui (Nuin 2007), combined with MrModelTest and Paup, was utilised to determine the best-fit evolution model for each locus using the Akaike Information Criterion (AIC). BI was conducted with six simultaneous MCMC chains, and trees were sampled every 100th generation. The analyses were stopped after 5,000,000 generations when the average standard deviations of the split frequencies were below 0.01. The first 25% of the resulting trees were discarded as burn-in and PP was calculated from the remaining sampled trees. The phylogenetic tree was visualised using FigTree version 1.4.0 (http://tree.bio.ed.ac.uk/software/figtree/).

Taxon treatment

Papiliomyces longiclavatus Y. Zhang, Y.P. Xiao & T.C. Wen, sp. nov.

- IndexFungorum IF558796

Materials

Holotype:

a. scientificName: ***Papiliomyces longiclavatus***; country: China; stateProvince: Guizhou; county: Guiyang City; locality: Yangchang Town; verbatimElevation: 1303 m;

verbatimCoordinates: 26°50′12.23″N, 106°53′41.58″E; decimalLatitude: 0.836731; decimalLongitude: 106.894883; georeferenceProtocol: label; eventDate: 14 June 2020; lifeStage: sexualMorph; catalogNumber: GACP YC20061403; recordedBy: Yan Zhang; identifiedBy: Yuan-pin Xiao; dateIdentified: 2020; occurrenceID: 94F0EF70-F2D9-5663-BB82-44C056D5B97A; ex-type: GZUCC-1403

Paratype:

a. scientificName: ***Papiliomyces longiclavatus***; country: China; stateProvince: Guizhou; county: Guiyang City; locality: Yangchang Town; verbatimElevation: 1325.7 m; verbatimCoordinates: 26°50′12.03″N, 106°53′41.70″E; decimalLatitude: 0.836675; decimalLongitude: 106.894917; georeferenceProtocol: label; eventDate: 14 June 2020; lifeStage: sexualMorph; catalogNumber: HKAS 115914; recordedBy: Yan Zhang; identifiedBy: Yuanpin Xiao; dateIdentified: 2020; occurrenceID: BA6BD204-6AB6-58CF-9EA3-850CB1357663

Description

Facesoffungi number: FoF 10474

Sexual morph (Fig. 1): Host: a bat moth larva (Lepidoptera, Hepialidae), 3.5–4.8 cm long, greyish to light yellow. Stromata: 4–6 cm long, 0.3–0.5 cm wide, arising from the head of host, clavate, solitary. Stipe: cylindrical, greyish to light yellow, fleshy, glabrous, enlarging abruptly at fertile portion. Fertile head: 1.5–2.1 cm long, 0.4–0.6 cm wide, grey white to dark grey, different from the stipe, without sterile tip. Ascomata: 320–580 × 110–230 μm (442 × 186 μm, n = 30), flask-shaped, immersed. Asci: 140–230 × 5–7 μm (183 × 6 μm, n = 30), narrowly cylindrical, 8-spored, hyaline, with a thick apical cap. Apical cap: 5–7 μm (6 μm, n = 30). Ascospores as long as asci, hyaline, filiform, smooth, irregularly breaking into secondary spores. Secondary spores: 2–9 × 1–2 μm (5.5 × 1.5 μm, n = 30), cylindrical, hyaline, irregular length.

Asexual morph (Fig. 2): Colonies on Czapek agar: attaining a diameter of 2–3 cm within 14 d at 25°C, dense, flat, velvety, white. α-phialides: 13–24 × 1–2 μm (18 × 1.5 μm, n = 30), hyaline, *Hirsutella*-like smooth, solitary, mostly arising from aerial hyphae, slender, with a short neck. β-phalides: 28–45 × 1–2 μm (36 × 1.5 μm, n = 30), hyaline, smooth, slender, *Acremonium*-like, mostly solitary. α-conidia: 3–5 × 1–3 μm (4.5 μm, n = 30), subglobose, one-celled, smooth, hyaline. β-conidia: 6–10 × 1–3 μm (8 × 2 μm, n = 30), fusiform, with both ends sharp, one-celled, smooth.

Host: On larvae of a bat moth (Lepidoptera, Hepialidae) living in soil.

Etymology

Referring to the shape of the stroma.

Distribution

Thus far only known from China.

Analysis

Phylogeny

Ten taxa (two with new sequence data) were included in the combined *ITS*, *SSU*, *TEF-1α*, *RPB1*, *LSU* and *RPB2* dataset (Table 1), which included 5016 characters with gaps: 561 characters for *ITS*, 887 for *LSU*, 1040 for *SSU*, 655 for *RPB1*, 957 for *RPB2* and 916 for *TEF-1α*. The IQ-TREE analysis had the same topology as the Bayesian analysis. The ML tree with the highest likelihood value, -9176.099, is presented. The matrix contained 280 unique alignment patterns, including 289 parsimony-informative, 133 singleton sites and 4594 constant sites. For the IQ-Tree, the respective partition best-fit models were: JC+I for *SSU* and *RPB2*, TNe for *LSU*, K2P for *ITS*, TN+F for *TEF-1α* and K2P+I for *RPB1*. In the Bayesian analysis, the respective partition best-fit models were: F81+I for *SSU*, GTR for *LSU* and *TEF-1α*, K80+G for *ITS* and *RPB1* and SYM for *RPB2*.

Discussion

Using morphological and phylogenetic analyses, we propose *Papiliomyces longiclavatus* sp. nov. from China. It shares a close relationship with *Papiliomyces liangshanensis* (EFCC 1452, EFCC 1523, Sung et al. (2007), Mongkolsamrit et al. (2020)), *Papiliomyces shibinensis* (Wen et al. 2015) and *Paecilomyces verticillatus* (Li et al. 2006). *Papiliomyces liangshanensis* was reclassified as *Ophiocordyceps liangshanensis* after morphological and phylogenetic analyses (Wang et al. 2021). However, the Nepalese collections (EFCC 1452, EFCC 1523) are lacking a morphological description (Sung et al. 2007) and which are named *Papiliomyces liangshanensis*. These two collection groups place our new species within the same clade (Fig. 3).

Phylogenetically, they are different from *Papiliomyces liangshanensis* (EFCC 1452, EFCC 1523): 0 bp in ITS, 0 bp in LSU, 4 bp/762 bp (99%) in TEF and 7 bp/762 bp (99%) in RPB2. However, the Nepalese collections (EFCC 1452, EFCC 1523) lack morphological descriptions (Sung et al. 2007) and which was then named *Papiliomyces liangshanensis*. Consequently, we indicated these two collections on the phylogenetic tree. These two collections, EFCC 1452 and EFCC 1523, require information about detection and morphology.

Furthermore, *Papiliomyces longiclavatus* is similar to *Papiliomyces shibinensis* in that it has clavate stromata with cylindrical stipe, immersed perithecia and filiform ascospores. However, it differs from *Papiliomyces shibinensis* in that it produces longer ascospores, cylindrical secondary ascospores, two types of phialides and two types of conidia (Table 2). It differs from *Paecilomyces verticillatus* in that it produces longer phialides, longer α-conidia and longer β-conidia. In the phylogenetic tree, *Papiliomyces longiclavatus* is distinct from *Papiliomyces shibinensis* and *Paecilomyces verticillatus*, which cluster in

different clades (Fig. 3). Thus, *Papiliomyces longiclavatus* is a distinct *Papiliomyces species* (Table 2).

Acknowledgements

This work was supported by the Science and Technology Foundation of Guizhou Province (No. [2019]2451-3) and the National Natural Science Foundation of China (No. 31760014). Fengyao Long was thanked for helping to sequence the specimens.The editor and reviewers were appreciated for the positive and constructive comments and suggestions.

References

- Alzohairy AM (2011) BioEdit: an important software for molecular biology. GERF Bulletin of Biosciences 2 (1): 60-61.
- Capella-Gutiérrez S, Silla-Martínez J, Gabaldón T (2009) trimAl: a tool for automated alignment trimming in large-scale phylogenetic analyses. Bioinformatics 25 (15): 1972-1973. https://doi.org/10.1093/bioinformatics/btp348
- Castlebury LA, Rossman AY, Sung GH, Hyten AS, Spatafora JW (2004) Multigene phylogeny reveals new lineage for *Stachybotrys chartarum*, the indoor air fungus. Mycological Research 108 (8): 864-872. https://doi.org/10.1017/S0953756204000607
- Cheek M, Nic Lughadha E, Kirk P, Lindon H, Carretero J, Looney B, Niskanen T, et al. (2020) New scientific discoveries: Plants and fungi. Plants, People, Planet 2 (5): 371-388. https://doi.org/10.1002/ppp3.10148
- Hoang DT, Chernomor O, von Haeseler A, Minh BQ, Vinh LS (2018) UFBoot2: Improving the ultrafast bootstrap approximation. Molecular Biology and Evolution 35: 518-522. https://doi.org/10.1093/molbev/msx281
- Hopple JS (1994) Phylogenetic investigations in the genus *Coprinus* based on morphological and molecular characters. Duke University
- Hywel-Jones NL (1994) *Cordyceps khaoyaiensis* and *C. pseudomilitaris*, two new pathogens of lepidopteran larvae from Thailand. Mycological Research 98 (8): 939-942. https://doi.org/10.1016/S0953-7562(09)80267-0
- Jayasiri SC, Hyde KD, Ariyawansa HA, Bhat J, Promputtha I (2015) The faces of Fungi database: fungal names linked with morphology, phylogeny and human impacts. Fungal Diversity 74 (1): 3-18. https://doi.org/10.1007/s13225-015-0351-8
- Kalyaanamoorthy S, Minh BQ, Wong T, Haeseler AV, Jermiin LS (2017) ModelFinder: Fast model selection for accurate phylogenetic estimates. Nature Methods 14 (6). https://doi.org/10.1038/nmeth.4285
- Katoh K, Standley D (2013) MAFFT multiple sequence alignment software version 7: improvements in performance and usability. Molecular Biology and Evolution 30 (4): 772-780. https://doi.org/10.1093/molbev/mst010
- Kepler RM, Sung GH, Ban S, Nakagiri A, Chen MJ, Huang B, Li Z, Spatafora JW (2012a) New teleomorph combinations in the entomopathogenic genus *Metacordyceps*. Mycologia 104 (1): 182-197. https://doi.org/10.3852/11-070

- Kepler RM, Sung GH, Harada Y, Tanaka K, Tanaka E, Hosoya T, Bischoff JF, Spatafora JW (2012b) Host jumping onto close relatives and across kingdoms by *Tyrannicordyceps* (Clavicipitaceae) gen. nov. and *Ustilaginoidea* (Clavicipitaceae). American Journal of Botany 99 (3): 552-561. https://doi.org/10.3732/ajb.1100124
- Kepler RM, Humber RA, Bischoff JF, Rehner SA (2014) Clarification of generic and species boundaries for *Metarhizium* and related fungi through multigene phylogenetics. Mycologia 106 (4): 811-829. https://doi.org/10.3852/13-319
- Liu YJ, Whelen S, Hall BD (1999) Phylogenetic relationships among ascomycetes: evidence from an RNA polymerse II subunit. Molecular Biology & Evolution 16 (12): 1799-1808. https://doi.org/10.1093/oxfordjournals.molbev.a026092
- Li Z, Han Y-F, Liang Z-Q, et al. (2006) *Paecilomyces verticillatus*, a new species isolated from soil in China. Mycotaxon 95: 133-136.
- Minh BQ, Schmidt HA, Chernomor O, Schrempf D, Lanfear R, et al. (2020) Corrigendum to: IQ-TREE 2: New models and efficient methods for phylogenetic inference in the Genomic Era. Molecular Biology and Evolution 37 (8). https://doi.org/10.1093/molbev/msaa015
- Mongkolsamrit S, Khonsanit A, Thanakitpipattana D, Tasanathai K, Luangsa-Ard J (2020) Revisiting *Metarhizium* and the description of new species from Thailand. Studies in Mycology 95 https://doi.org/10.1080/12298093.2021.1923388
- Mueller GM, Schmit JP, et al. (2007) Fungal biodiversity: what do we know? What can we predict? Biodiversity and Conservation 16 https://doi.org/10.1007/s10531-006-9117-7
- O'Donnell K, Sarver BAJ, Brandt M, Chang DC, Noble-Wang J, Park BJ, Sutton DA, Benjamin L, Lindsley M, Padhye A (2007) Phylogenetic diversity and microsphere array-based genotyping of human pathogenic *Fusaria*, including isolates from the multistate contact lens-associated U.S. keratitis outbreaks of 2005 and 2006. Journal of Clinical Microbiology 45 (7): 2235-2248. https://doi.org/10.1128/JCM.00533-07
- Ronquist F, Teslenko M, Mark P, Ayres DL, Darling A, Höhna S, Larget B, Liang L, Huelsenbeck S (2012) MrBayes 3.2: Efficient Bayesian phylogenetic inference and model choice a large model space. Systematic Biology 61 (3): 539-542. https://doi.org/10.1093/sysbio/sys029
- Sorokin N (1883) Plant parasites causing infectious diseases of man and animals. Vol. 2. Edition of the Chief Military Medical Directorat, St Petersburg, 168-169 pp.
- Sung GH, Sung J-M, Hywel-Jones NL, Spatafora JW (2007a) A multi-gene phylogeny of Clavicipitaceae (Ascomycota, Fungi): identification of localized incongruence using a combinational bootstrap approach. Molecular Phylogenetics & Evolution 44 (3): 1204-1223. https://doi.org/10.1016/j.ympev.2007.03.011
- Sung GH, Hywel-Jones NL, Sung JM, Luangsa-Ard JJ, Spatafora JW (2007b) Phylogenetic classification of *Cordyceps* and the clavicipitaceous fungi. Studies in Mycology 57 (1): 5-59. https://doi.org/10.1016/S0166-0616(14)60128-7
- Vilgalys R, Hester M (1990) Rapid genetic identification and mapping of enzymatically amplified ribosomal DNA from several *Cryptococcus* species. Journal of Bacteriology 172 (8): 4238-4246. https://doi.org/10.1128/jb.172.8.4238-4246.1990\
- Wang Y, Dai YD, Yang ZL, Guo R, Yu H (2021) Morphological and molecular phylogenetic data of the Chinese medicinal fungus *Cordyceps liangshanensis* reveal its new systematic position in the family Ophiocordycipitaceae. Mycobiology 49 (4): 297-307. https://doi.org/10.1080/12298093.2021.1923388

- Wen TC, Zha LS, Xiao YP, Wang Q, Kang JC, Hyde K (2015) *Metacordyceps shibinensis* sp. nov. from larvae of Lepidoptera in Guizhou Province, southwest China. Phytotaxa 226 (1): 51-62. https://doi.org/10.11646/phytotaxa.226.1.5
- White T, Bruns T, Lee S, Taylor F, White T, Lee SH, Taylor L, Shawetaylor J (1990) Amplification and direct sequencing of fungal ribosomal RNA genes for phylogenetics. PCR protocols: a guide to methods and applications. Academic Press315-322. https://doi.org/10.1016/B978-0-12-372180-8.50042-1
- Wijayawardene NN, Hyde KD, Lumbsch HT, Jian KL, Phookamsak R (2018) Outline of Ascomycota: 2017. Fungal Diversity 88 (2): 167-263. https://doi.org/10.1007/s13225-018-0394-8
- Yang Y, Xiao YP, Yu GJ, Wen TC, Deng CY, Meng J, Lu ZH, et al. (2021) *Ophiocordyceps aphrophoridarum* sp. nov., a new entomopathogenic species from Guizhou. Biodiversity Data Journal 9: 66115. https://doi.org/10.3897/BDJ.9.e66115
- Zang M, Liu DQ, Hu RY (1982) Notes concerning the subdivisions of *Cordyceps* and a new species from China. Acta Botanica Yunnanica 4 (02): 1-3. URL: https://journal.kib.ac.cn/EN/Y1982/V4/I02/1

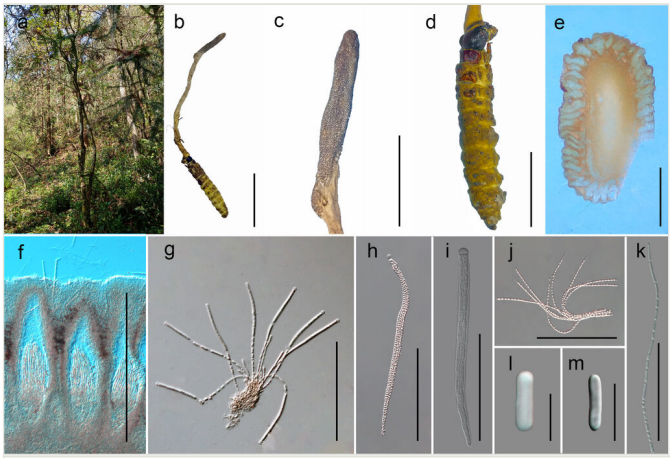

Figure 1.

Papiliomyces longiclavatus (GACP YC20064103), sexual morph. **a** Habitat; **b** Overview of the host and stroma; **c** Stroma; **d** Host; **e, f** Vertical section of the stroma; **g, h** Immature to mature asci; **i** Apical cap; **j, k** Part of ascospores; **l, m** Secondary spores. Scale bars: b = 3 cm, c = 1 cm, d = 1 cm, e = 0.1 cm, f = 400 µm, g = 150 µm, h–j = 100 µm, k = 50 µm, l, m = 5 µm.

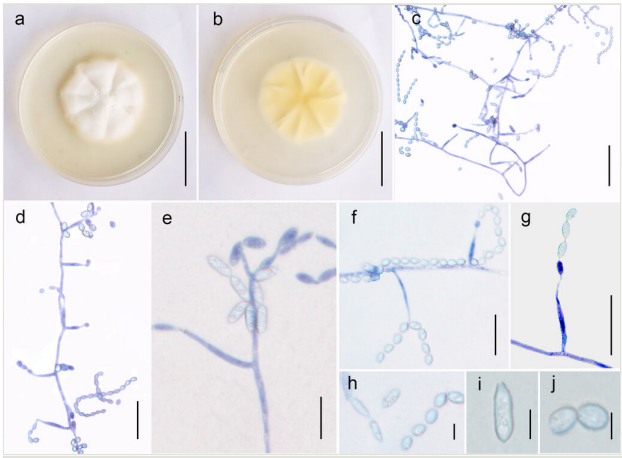

Figure 2.

Papiliomyces longiclavatus (ex-type: GZUCC-4103), asexual morph. **a** Upper side of the culture; **b** Reverse of the culture; **c** Mycelium with phialides and conidia; **d, f** α-phialides; **e, g** β-phialides; **h** Two types of conidia; **i** β-conidia; **j** α-conidia. Scale bars: a, b = 1 cm, c = 30 μm, d–g = 20 μm, h–j = 5 μm.

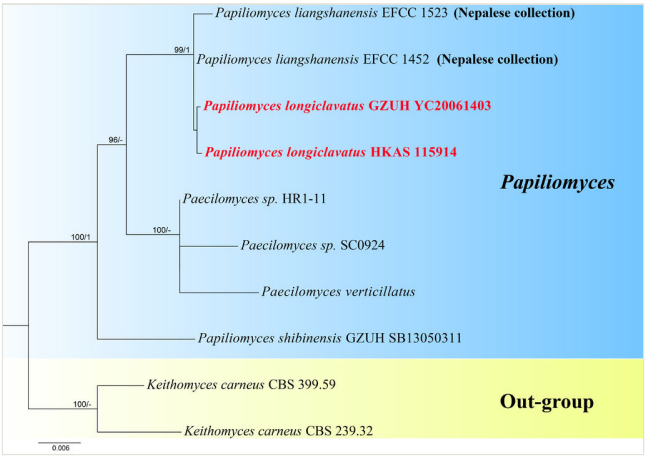

Figure 3.

Phylogram of *Papiliomyces longiclavatus* generated from the Maximum Likelihood (IQ-tree) analysis of combined *ITS*, *SSU*, *TEF-1α*, *RPB1*, *LSU* and *RPB2* sequence data. The tree was rooted to *Keithomyces carneus* (CBS 399.59) and *Keithomyces carneus* (CBS 239.32). Maximum Likelihood bootstrap values greater than 75% and posterior probabilities from Bayesian Inference more than 0.95 were indicated above the nodes. The new species is indicated in red.

Table 1.

List of taxa and their GenBank accession numbers used in this study.

Species	Strains	Locality	Substrate	*SSU*	*LSU*	*TEF-1 α*	*RPB1*	*RPB2*	*ITS*	
Keithomyces carneus	CBS 399.59	USA	Soil	EF468989	EF468842	EF468788	EF468895	EF468939	MT078887	S e (
Keithomyces carneus	CBS 239.32	France	Sand dune	EF468988	EF468843	EF468789	EF468894	EF468938	AY624171	S e (
Paecilomyces sp.	HR1-11	South Korea	Cymbidium kanran						KU141150	P e (
Paecilomyces sp.	SC0924	China	Soil						KR011745	X (
Paecilomyces verticillatus									DQ836182	P (
Papiliomyces liangshanensis	EFCC 1523	Korea	Lepidoptera	EF468961	EF468814	EF468755	–	EF468918	–	S (
Papiliomyces liangshanensis	EFCC 1452	Korea	Lepidoptera	EF468962	EF468815	EF468756	–	–	–	S (
Papiliomyces longiclavatus	GZUH YC20061403	China	Lepidopteran larva	MZ702112	MZ702101	MZ955880	MZ955876	OM419142	MZ702080	T
Papiliomyces longiclavatus	HKAS 115914	China	Lepidoptera larva	MZ702114	MZ702103	MZ955882	MZ955878	OM419143	MZ702082	T
Papiliomyces shibinensis	GZUH SB13050311	China	Lepidoptera	KR153588	–	KR153589	KR153590	–	–	W (

Table 2.

Synopsis of *Papiliomyces* species discussed in the paper.

Species	*Papiliomyces shibinensis*	*Paecilomyces verticillatus*	*Papiliomyces longiclavatus*
Stromata	Stromata 42 mm long, 2–3 mm wide, growing from the head of Lepidoptera larva, simple.		Stromata arising from the head of host, ovary, clavate, solitary, 40–60 mm long, 3–5 mm thick.
Stipe	Stipe 17–20 mm long, 2–3 mm wide, flexuous, white to faint yellow.		Stipe cylindrical, greyish-white to light yellow, fleshy, glabrous, enlarging abruptly at fertile portion.
Fertile part	Fertile part on the upper 50% of the stromata, 18–22 mm long, 2–3 mm wide, cylindrical or obtuse, faint yellow, differentiated from stipe, without a sterile apex.		Fertile head length 15–21 mm, 4–6 mm thick, grey white to grey black, mature with a clear boundary with the stalk, no sterile tip.
Perithecia	Ascomata crowded, completely immersed, ampulliform, ovoid to oblong, 630–830 × 240–340 µm, curved, with the ostioles opening on the surface of the fertile head.		Ascomata, bottle-shaped, buried, 320–580×110–230 µm
Asci	Asci 130–200 × 5.1–8.3 µm, 8–spored, hyaline, cylindrical, with a prominent apical cap; apical cap 4.7–5.9 × 2.8–3.5 µm		Asci, narrowly cylindrical, 8-spored, hyaline, possessing a prominent apical cap, 140–230×4.8–6.5 µm
Ascospores	Ascospores 120–170 × 1.4–2.1 µm, hyaline, filiform, smooth–walled, multiseptated with cells 4–5.6 µm long.		Ascospores are nearly isometric, transparent and colourless, slender, filiform, smooth, mature and break into secondary ascospores.
Part–spores	Not breaking into secondary ascospores.		Secondary ascospores, 5.2–9.3 × 1.1–1.5 µm
Condiophores	Conidiophores short, hyaline, smooth, up to 60 µm long, mostly arising from aerial hyphae.	Conidiophores hyaline, 9.6–19.8 µm. Phialides 7.8–14.4 × 1.2–2.4 µm, awl–shaped or consisting of a cylindrical basal portion and a thin neck	Two types of phalides: α–phalides and β–phalides. α–phialides 12.6–23.8 × 1.4–2.4 µm, hyaline, smooth, solitary, mostly arising from aerial hyphae, shorter and gradually thinner upwards. β–phalides 28.2–44.5 × 1.2–1.8 µm hyaline, smooth, slender, conical, mostly solitary.
Conidia	Conidia ellipsoidal, ovoid or fusiform, 1–celled, 3.5–5 × 2–3 µm, in long divergent, dry chains.	Conidia hyaline, mostly subglobose to ellipsoidal, 1.2–1.8 × 0.6–1.2 µm; few fusiform, 1.8–3.0 × 1.8–2.4 µm, forming divergent, dry chains or aggregating spore group	α–conidia.1–5.1×1.2–2.5 µm, round, single celled, smooth, colourless and transparent. β–conidia 5.8–9.9×1.3–2.7 µm, fusiform, with sharp ends, single cell and smooth wall.

Reference	Wen et al. (2015)	Li et al. (2006)	This study